Solid Freeform Fabrication 2024: Proceedings of the 35th Annual International Solid Freeform Fabrication Symposium – An Additive Manufacturing Conference
Reviewed Paper

PERFORMANCE ANALYSIS OF SELECTIVE SEPARATION SHAPING LARGE-SCALE POWDER BONDING TECHNOLOGY

Xiang Gao*, Behrokh Khoshnevis†
* Amazon Inc
†University of Southern California

Abstract

Selective Separation Shaping (SSS) has proven effective in additive manufacturing (AM) for metals, polymers, and cementitious materials. Recent advancements in thick layer deposition have extended its application to large-scale product fabrication. Achieving high efficiency in SSS is critical for producing large cementitious parts. This study examines the integration of vibration and airflow to improve powder deposition stability and explores the relationship between deposition volume and nozzle movement speed. The optimized building speed of SSS is then presented and compared to existing commercial AM technologies.

Keywords Additive manufacturing, powder deposition, building speed

1. Introduction

1.1 Additive manufacturing

Additive manufacturing, commonly known as 3D printing, builds a 3D part by adding material layer by layer, following the pattern generated from a CAD model. This technology has demonstrated its capabilities in fabricating metal, polymer, composite materials, and more [1]. Recently, the application of AM for large-scale fabrication has garnered increasing attention. Some technologies for large-scale production are essentially scaled-up versions of their original methods.

Several AM technologies have the potential to fabricate large parts:

The Fortus 900 [2] is the largest FDM printer produced by Stratasys, capable of manufacturing products within a 36 x 24 x 36-inch build volume. This technology offers advantages such as high product quality, the ability to create thin structures (as small as 0.007 inches) [3], and relatively fast build speeds. However, it is limited in its ability to construct larger structures and has a restricted range of material options.

The S-Max [4] is a binder jetting [5] 3D printer developed by ExOne, primarily focused on applying binder jetting technology to sandcasting foundries. It features a relatively large build volume of 70.9 x 30.4 x 27.6 inches.

Contour Crafting (CC), introduced by Dr. Behrokh Khoshnevis [6-8], is the first process with the potential to build large-scale structures. CC is based on the extrusion of concrete materials. In this process, a path plan file is transferred to the machine's controller, and the machine then

extrudes semi-fluid concrete through a specially designed nozzle, following the planned path. The next layer is deposited after the preliminary hardening of the previous one. With its relatively fast build speed, structural strength, and flexible construction capabilities, this technology holds significant potential for use in the construction of buildings, infrastructure, and even planetary structures.

D-Shape technology, invented by Enrico Dini [9], is designed for fabricating large-scale art sculptures using environmentally friendly materials. The process utilizes binder jetting and solidifies magnesium oxide in the presence of magnesium hexahydrate. A key advantage of this technology is that the sand volume serves as a support structure, enabling the fabrication of relatively complex shapes with overhangs. Additionally, it uses eco-friendly materials. However, when it comes to large-scale manufacturing, the cost of this process is still not as competitive as extrusion-based technologies like Contour Crafting.

1.2 Selective Separation Shaping

A significant class of AM processes is based on powder materials; however, all of these processes have been limited to sub-millimeter powder layers [10]. Selective Separation Shaping (SSS) is a new, versatile powder-based AM process that has demonstrated the ability to build meso-scale metallic and ceramic parts [11]. Now, its potential to break the scale barrier in powder-based processes is being proven [12].

Our experiments show that SSS, unlike traditional AM technologies [13,14], is the first powder-based process capable of building layers that are several centimeters thick. SSS also produces parts with exceptional surface quality at unprecedented fabrication speeds. This study focuses on the fabrication of cementitious composite parts, presenting the results of experiments using Portland cement, Sorel cement, and gypsum.

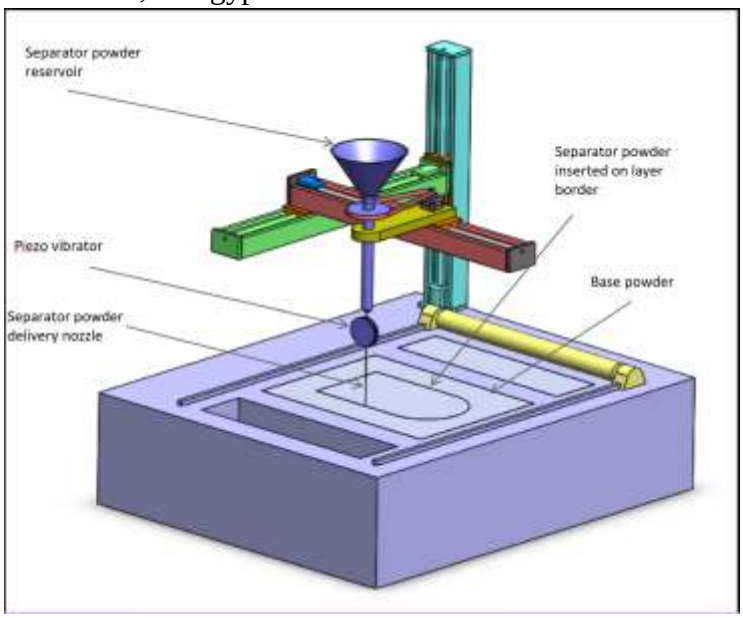

Figure 1. The image shows nozzle system within the SSS machine, with the nozzle inserted into the base powder.

In the meso-scale sintering-based SSS process, recently reported in the literature, a thin wall of high-melting-point separator powder (S-powder) is deposited within the base material powder (B-powder) to form a barrier at the boundary of each layer. Figure 1 illustrates the concept of the SSS process. This barrier creates a separation between the part and the surrounding material, allowing for easy removal of the part after sintering is complete. The part is then removed from the platform and placed into a sintering furnace. After sintering, the part is easily separated from the surrounding powder, as the S-powder remains in its powder state due to its higher sintering temperature. In the extended SSS process for large-scale part fabrication, the thickness of each progressive powder layer is significantly greater than in meso-scale fabrication.

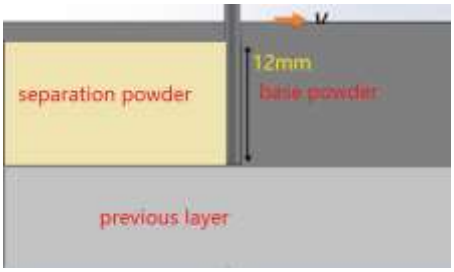

Figure 21. Deposition of thin wall of separating powder on a layer with 12mm thickness

In the first step of the process, a uniform layer of base powder is spread across the build tank. The nozzle is then inserted into the base powder, depositing the S-powder along the layer contour. Afterward, the nozzle is raised, and another layer of base powder is spread over the previous one. This process repeats until all layers are completed. At this point, a sufficient amount of bonding liquid—such as water for hydraulically activated cementitious powders—is applied to the top layer. The liquid gradually permeates downward through gravity and capillary action, initiating part consolidation through chemical bonding. Depending on the choice of base material, the initial weak consolidation phase may be completed within several hours, after which the part will be strong enough to be removed from the build tank. The entire material block, where the base and separation materials remain together, is then placed in a controlled environment for further consolidation. Finally, the part is separated from the base material.

As we can see from the SSS process, two factors can be accelerated to increase overall efficiency. The first is the separation powder deposition speed; if this can be improved, the entire process will become faster. The second is the nozzle movement speed, which can be optimized in relation to the deposition rate. This paper will discuss the separation flow deposition process, which determines the overall build speed.

1.3 Advantages of Selective Separation Shaping

Figure 3 shows the alpha machine, which serves as a proof-of-concept for the SSS process in fabricating large cementitious parts.

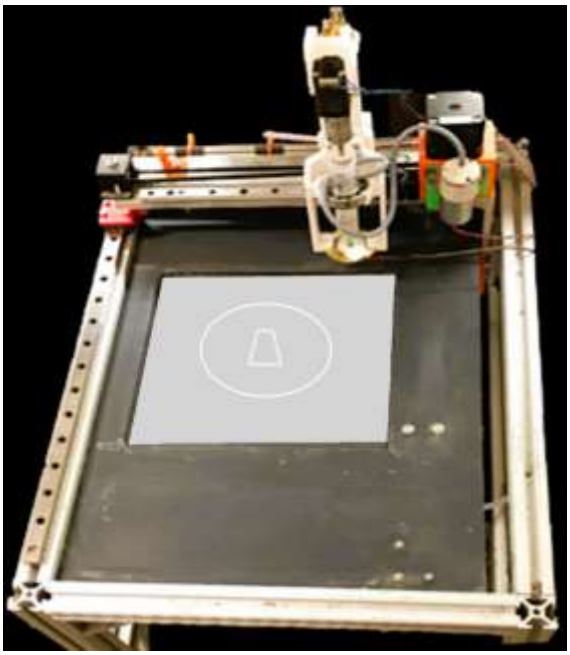

Figure 3. Selective Separation Shaping prototype

High speed: With the ability to increase layer thickness without limitation (currently up to 24 mm), SSS can complete fabrication with fewer layers, significantly reducing time and cost.

Good surface quality: The surface quality of parts produced by SSS can achieve a high standard without the need for post-processing.

Material flexibility: With a single platform, parts can be fabricated using various materials, such as cement, magnesium-based sand, plaster, zirconia, and more.

2. Samples built with SSS in different materials

2.1. Portland Cement

The first material tested was Portland cement due to its widespread use in infrastructure construction projects. The solidification process of hydraulic cement is complex, involving numerous physical and chemical reactions. Significant effort has been invested in identifying the optimal parameters for the SSS cement curing process, as traditional water-cement mixing does not occur in SSS. The part shown in Figure 4 was built in 20 minutes, with a petal shape thickness of 22 mm. The surface quality of the single layer is quite good.

Figure 4. Single-layer (above) and double-layer (below) Portland cement parts made by SSS

2.2. Gypsum

The gypsum used in this study is Plaster of Paris from DAP Co., selected for its high quality and wide range of applications. The result of the gypsum printing using SSS is shown in Figure 5.

Figure 5. Gypsum parts made by SSS

The single-layer gypsum petal, 10 mm high, was printed in 13 minutes. After two hours of solidification, the part was separated from the surrounding material. The gypsum parts exhibited some surface cracks, likely due to rapid evaporation and the heat generated by chemical reactions during the hydration process. Several experiments were conducted to determine optimal parameters, such as water particle size and flow rate, as these factors directly impact the part's surface smoothness by affecting the interaction between water and the base material during manufacturing. Further analysis is needed, as water penetration into gypsum is very low and gypsum shrinkage varies in different directions.

2.3. Magnesium-based material

Magnesium oxychloride is a compound formed from magnesium chloride ($MgCl_2$) and magnesium oxide (MgO). It can achieve relatively high strength and has an attractive appearance, making it a promising candidate material for the SSS process. The chemical reaction formula between $MgCl_2$ and MgO is shown below [15]:

$$2MgCl_2 + 6MgO + nH_2O = 3Mg(OH)_2 \cdot MgCl_2 \cdot nH_20 + 5Mg(OH)_2 \cdot MgCI_2 \cdot nH_2$$

$Equation\ 1$

Figure 6. Magnesium-based part made by SSS

First, Magnesium Oxide (with a purity of 98%, obtained from SIGMA-ALDRICH) is mixed with sand (200 to 400 microns from ACTIVE PRODUCTS, INC.) in a weight ratio of 1 to 2. Next, a calculated amount of Magnesium Chloride (99.9% Hexahydrate, $MgCl_2 \cdot 6H_2O$ from SIGMA-ALDRICH) is added to the solution based on a molar ratio of 7.5. This solution is then sprayed onto the base material to generate Magnesium Chloride. After two days of reaction between $MgCl_2$ and MgO, the part is solidified, and the desired component is separated from the remaining base material. As shown in Figure 6, the surface quality of the part is relatively rough due to interference between the sand in the magnesium oxide powder and the outer separation and covering sand. Despite the specimens demonstrating relatively high strength, this material is not considered ideal for SSS applications due to its high cost and chemical instability when exposed to other powders.

3. Separation powder deposition improvement

The surface quality of parts built by SSS largely depends on the quality of the separation powder (soda lime) deposition. If the powder deposition is insufficient, a solid separation wall may not be formed or may be produced with low quality, which impairs soda lime's ability to maintain the part's shape and dimensions close to specifications.

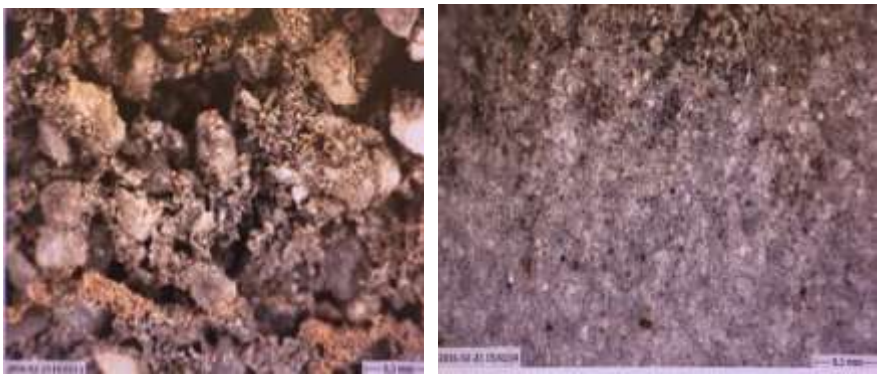

Figure 7. Left: Cross section of layer without sufficient soda lime as S powder; Right: Cross section of layer with sufficient S powder

Figure 7 shows a comparison between surfaces with and without sufficient S-powder deposition. The top picture clearly demonstrates that the surface quality with adequate S-powder deposition is significantly better than that of surfaces resulting from insufficient S-powder deposition.

The quality of soda lime deposition has a considerable impact on building speed, as the printing head's movement must be slowed if the deposition flow is inadequate to fill the entire separation slot.

To ensure sufficient deposition, it is crucial to maintain a stable deposition flow and prevent the S-powder from clogging in the powder container, which is a common issue in powder flow situations [15].

The causes of clogging in the deposition process identified through experiments are: 1) Contamination within the S-powder due to the lack of a seal between the powder container and syringe, and 2) Formation of arches in the powder during deposition due to gravity, which can obstruct the flow of powder, as shown in Figure 8.

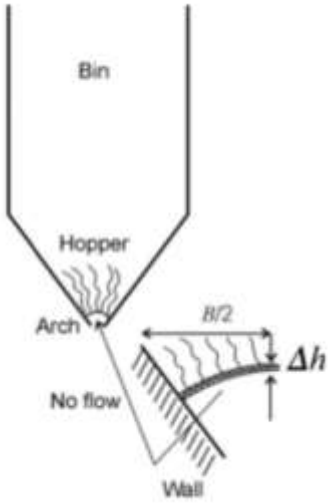

Figure 8. Plot of arch generation inside the syringe [13]

To address the first issue, a sieving stage has been introduced before filling the syringe with S-powder to prevent contamination. To tackle the second issue, both aggressive vibration and airflow directed at the bottom of the hopper are used to dislodge any formed arches.

Given that the hopper used in SSS is small, the vibration method was initially implemented. After several experiments with piezoelectric vibration, an amplitude of 5 microns and a frequency of 2 kHz were successfully applied, effectively preventing arch formation. For increased deposition rates, airflow was applied to the upper side of the hopper containing the

S-powder. Experimental results showed that this method successfully mitigates low deposition rates caused by high-density powder particles. Additionally, a miniature pump was installed on the S-powder container to pressurize it and increase the outflow rate of the S-powder from the nozzle.

For increased deposition rate, airflow was applied to the upper side of the hopper containing the S-powder. The result of experiments showed that this method is capable of increasing low deposition rate caused by high density powder particles. To obtain stable and adequate S-powder deposition, a miniature pump with proper air pressure was installed on the S-powder container to pressurize the container and increase the outflow rate of the S-powder from the nozzle.

To evaluate the effects of key factors on deposition, a full factorial design experiment was developed and conducted. Three factors were analyzed based on previous experimental results and available lab equipment. As shown in Table 1, "A" represents the vibration of a cellphone vibrator, which has low frequency but high amplitude; "B" represents piezoelectric vibration, which has high frequency but low amplitude; and "C" represents airflow provided by a diaphragm pump. In the experiments, each factor was tested in two states: "+" indicates the presence of the element (e.g., airflow is applied), while "-" indicates its absence. Three replicates were performed for each condition, and the weight of the soda lime deposited within 300 seconds was recorded and marked as "Y" in Table 1.

The design table and results are presented in Table 1:

Table 1. The 2^3 full factorial design table

A	B	C	Y1/g	Y2/g	Y3/g
-	-	-	0	0	0
-	-	+	0	0	0
-	+	-	2.755	1.611	0.795
-	+	+	9.167	19.569	14.206
+	-	-	3.265	3.05	0.625
+	-	+	1.985	6.87	6.667
+	+	-	3.11	0.969	0.953
+	+	+	6.014	15.805	8.949

Based on the experimental results, half-normal plots for displacement and dispersion are generated to illustrate the significance of the parameters.

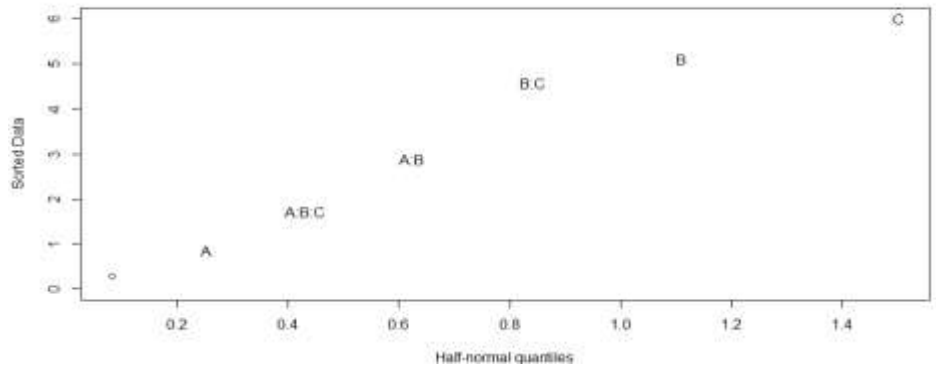

Figure 9. Half norm plot for dispersion of experiment results

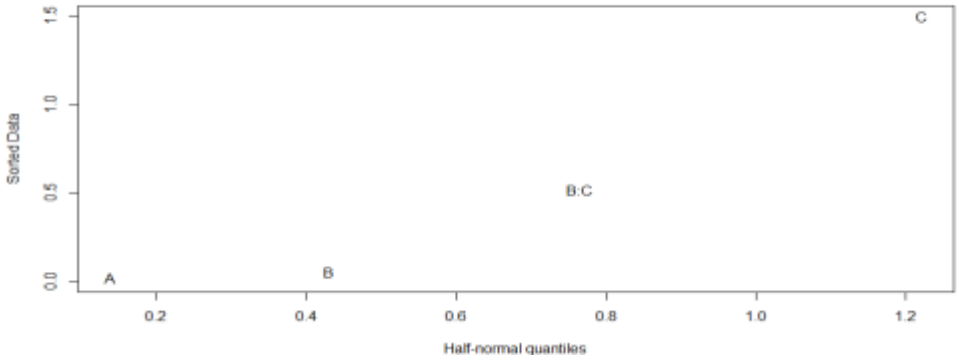

Figure 10. Half norm plot for variance of experiment results

From the two plots (Figures 9 and 10), it is evident that main factors B and C significantly affect the dispersion of deposition, while factor C and the interaction between B and C are crucial for changing the deposition quality. Additionally, regression models based on these significant factors were calculated. Following a two-step strategy, factors B and C are set to positive values, while factor A is set to negative, to achieve the maximum deposition amount with minimal energy cost and system complexity. The regression equations are shown below:

$$y = 4.432 + 2.560 \cdot B + 3.004 \cdot C$$

$Equation\ 2$

$$\sigma = 0.1924 + 0.7466 \cdot C + 0.2580 \cdot B \cdot C$$

$Equation\ 3$

In conclusion, the combination of piezoelectric vibration and airflow is introduced as an economical and efficient solution for ensuring stable and sufficient powder flow.

4. Potential of SSS on large-scale and complicated shape fabrication

SSS is believed to have significant potential for large-scale fabrication in construction and public art [16], owing to its layer-based process which enables the construction of 3D structures. This chapter will examine the speed of SSS and compare it to other commercial 3D printers to demonstrate its potential for large-scale product fabrication.

A key challenge in scaling small-scale fabrication technologies to large-scale applications is the slow building speed. This section will discuss the building speed of SSS at various layer thicknesses and compare it to Contour Crafting and D-Shape to highlight its potential for large-scale fabrication.

As mentioned, the current printing head allows SSS to produce high-quality parts with a layer thickness of 12.5 mm. In theory, the layer thickness in SSS can be increased indefinitely. To showcase the capability of SSS with increased layer thickness, a printing head with a 25.5 mm slot has been developed, as illustrated in Figure 11.

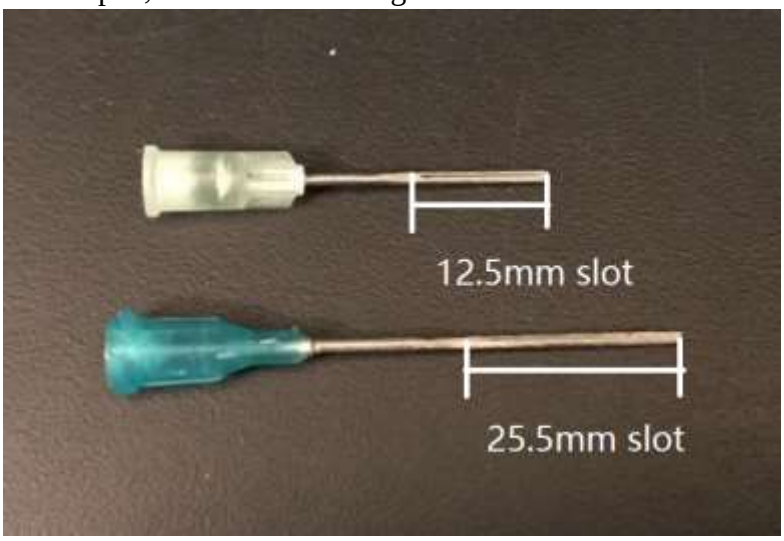

Figure 11. The upper printing head has a slot of 25.5mm high, and the lower printing head has a slot of 12.5mm high.

As shown in Figure 11, both the upper and lower needles have an outer diameter (OD) of 1.2 mm. The upper needle has a slot that is 25.5 mm long and 0.7 mm wide, while the lower needle features a slot that is 12.5 mm long and 0.7 mm wide.

4.1 Printing speed of SSS under different layer thicknesses

To ensure a smooth deposition flow, vibration and air pump settings are optimized to achieve the maximum separation powder deposition rate ($Rmax$) for various layer thicknesses. Additionally, several experiments were conducted to analyze the maximum printing speed, as

described by Equation 4, for different nozzles.

$$V_{max} = \frac{R_{max}}{\rho \cdot L \cdot D}$$

Equation 4

V_{max}: Maximum printing head moving speed (mm/s)

R_{max}: Maximum deposition rate (g/s)

ρ: Deposition of separation powder (g/mm^3)

L: Layer thickness (mm)

D: Diameter of nozzle (mm)

The first experiment tested the maximum moving speed of the head with a 12.5 mm slot. During the experiment, a 12 mm layer of cement was spread in the building tank, and the nozzle was inserted to begin depositing the separation powder. Various moving speeds were tested, revealing that the maximum moving speed for the head with the 12.5 mm slot is 18 mm/s. At this speed, the nozzle successfully forms a 1.2 mm tall separation gap filled with a sufficient amount of separation powder, as shown on the right side of Figure 12.

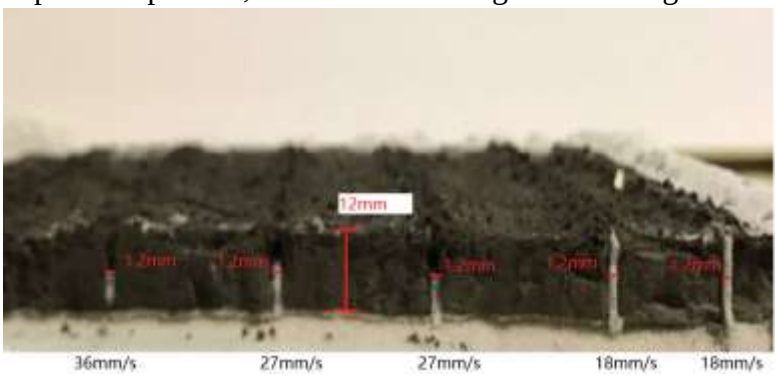

Figure 12. The gap formed by the nozzle with a 12.5mm slot a different moving speeds.

For the nozzle with a 25.5 mm slot, several moving speeds were tested, and the maximum moving speed was found to be 12 mm/s. Results for various moving speeds are shown in Figure 59.

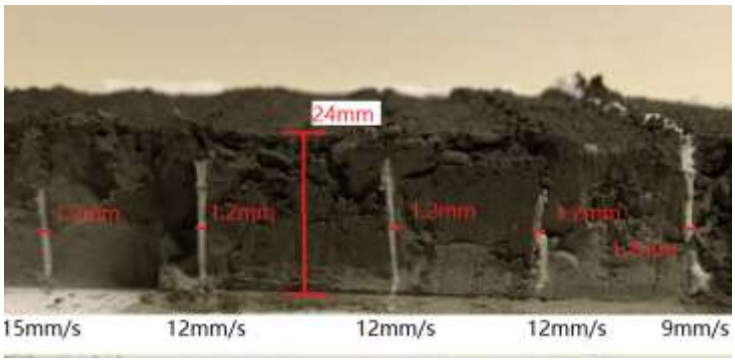

Figure 13. The gaps formed by the nozzle with a 25.5mm slot under different moving speeds.

Based on Table 2, the fabrication speed does not necessarily decrease by half when the layer thickness is doubled. This is because the maximum deposition rate can be increased by adjusting the vibration and air pump settings. For large-scale printing, the printing speed can be further enhanced as a larger printing head is used, allowing for a higher deposition rate. In conclusion, SSS can overcome limitations in printing speed for large-scale fabrication.

Table 2. The maximum printing speed of nozzles with different opening sizes.

Index	Opening height	Layer thickness	Maximum speed
1	12.5mm	12mm	18mm/s
2	25.5mm	24mm	12mm/s

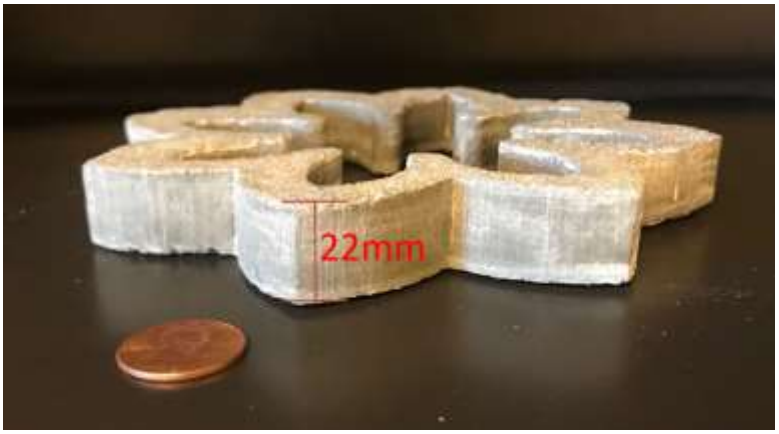

Figure 14. The image of a sample built with the layer thickness of 22mm.

A 22 mm thick sample, shown in Figure 14, was fabricated using the 25.5 mm head to demonstrate the surface quality of samples with greater layer thickness. The smooth surface of the sample indicates that the deposition of separation powder is adequate, as discussed in

Chapter 4. Comparing this sample to those shown in Chapter 2, it is evident that increasing the layer thickness in the SSS process does not negatively impact sample quality. Furthermore, it can be concluded that the SSS process is scalable for large-scale fabrication, as potential limitations related to fabrication speed and surface quality can be effectively addressed.

4.2 Comparison of SSS and commercialized mega-scale 3D-printing technologies

To demonstrate the capability of SSS in commercial large-scale fabrication, the building speed (Equation 5) of the current SSS machine is compared with that of commercial large-scale additive manufacturing machines.

$$T_{min} = \sum_{i=1}^{n}(\frac{p_i}{V_{max}} + w_i)$$

Equation 5

T_{min}: Total time needed for fabrication (s)

n: The total number of layers

p_i: The length of the trajectory that printing heads need to traverse in layer i (mm)

V_{max}: Maximum printing head movement speed (mm/s)

w_i: Pavement time (s) in layer i for powder-based printing

Contour Crafting [21] and D-Shape [22] are two commercialized technologies capable of large-scale fabrication. In the Contour Crafting process, the waiting time (w_i) between layers is negligible, as no pavement is required. In contrast, both SSS and D-Shape involve waiting times, but these are much shorter compared to the separation powder deposition time ($\frac{p_i}{V_{max}}$ $in\ Equation$ 5), particularly when the building pattern is significantly larger for large-scale fabrication. This study focuses solely on the separation powder deposition time. All fabrication parameters for the three additive technologies are compared in Table 3.

Table 3. The fabrication parameters of mega-scale 3D printing technologies.

Name	Nozzle movement speed	Layer thickness
Contour Crafting [15]	150mm/s	25-130mm
D-Shape [16]	100mm/s	5mm
SSS	12-18mm/s	No limitation (e.g., 12mm, 24mm)

Based on Table 3, the data indicates that the fabrication speed of SSS is comparable to that of D-Shape. Although the nozzle moving speed of SSS is 20% of that of D-Shape, the layer thickness of SSS is at least 500% greater. Currently, the printing speed of SSS is relatively slower than that of Contour Crafting. However, the speed of the SSS process can be significantly improved for larger-scale tasks by using a larger nozzle with a wider slot and higher flow rate of separation powder.

In conclusion, the current SSS technology is capable of completing large-scale fabrication jobs within a reasonable timeframe when compared to existing commercial technologies.

5. Conclusion

The current research represents a significant enhancement in the efficiency of Selective Separation Shaping (SSS) for cementitious materials. Two key approaches are implemented and discussed: first, the combination of airflow and piezoelectric vibration to improve powder flow deposition; and second, a strategy integrating powder deposition with nozzle moving speed. These methods are expected to reduce resource consumption and increase the reliability of SSS technology for cementitious part fabrication.

References

[1] Kaufui V. Wong and Aldo Hernandez, A Review of Additive Manufacturing, 17 June 2012, ISRN Mechanical Engineering Volume 2012, Article ID 208760.

[2] Stratasys F900 overview [Online]. Available: http://www.stratasys.com/3d-printers/production-series/fortus-900mc

[3] R. Noorani, Rapid Prototyping—Principles and Applications, John Wiley & Sons, 2006.

[4] S-max Tech Specs [Online]. Available: https://www.exone.com/Systems/Production-Printers/-S-Max

[5] K. Cooper, Rapid Prototyping Technology, Marcel Dekker, 2001.

[6] B. Khoshnevis, R. Dutton, Innovative rapid prototyping process makes large sized, smooth surfaced complex shapes in a wide variety of materials, Mater. Technol. 13 (2) (1998) 53–56.

[7] B. Khoshnevis, Automated construction by contour craftingrelated robotics and information technologies, Autom. ConStruct. 13 (1) (2004) 5–19.

[8] B. Khoshnevis, D. Hwang, K.T. Yao, Z. Yeh, Mega-scale fabrication by contour

crafting, Int.

J. Ind. Syst. Eng. 1 (3) (2006) 301–320.

[9] D shape [Online]. Available: http://d-shape.com/

[10] Nouri, H., and B. Khoshnevis. Study On Inhibition Mechanism of Polymer Parts in Selective Inhibition Sintering Process. Solid Free Form Fabrication Symposium, Austin, Texas 2015

[11] Zhang, J. and B. Khoshnevis, B. Selective Separation Sintering (SSS) – A new Additive Manufacturing Approach for metals and ceramics. Solid Free Form Fabrication Symposium,

Austin, Texas 2015

[12] B Khoshnevis, X Gao, B Barbara, H Nouri . Selective Separation Shaping (SSS)– Large- Scale Fabrication Potentials. Solid Free Form Fabrication Symposium, Austin, Texas 2017

[13] Hongxin Li, Xiaoyu Liang, Performance of High-Layer-Thickness Ti6Al4V Fabricated by Electron Beam Powder Bed Fusion under Different Accelerating Voltage Values, Materials, 2022

[14] Kietan Shergill, Yao Chen, Steve Bull, An investigation into the layer thickness efect on the mechanical properties of additively manufactured polymers: PLA and ABS, The International Journal of Advanced Manufacturing Technology, 2023

[15] Edwin S. Newman, A study of the system magnesium Oxide-Magnesium Chloride-Water and the heat of formation of Magnesium Oxychloride", Journal of Research of the National Bureau of Standards Vol. 54, No. 6, June 1955.

[16] X Gao. Selective Separation Shaping (SSS): Large Scale Cementitious Fabrication Potentials. USC 2019

[17] D. Hwang and B. Khoshnevis, Concrete wall fabrication by Contour Crafting, Dooil Hwang and Behrokh Khoshnevis, 2004.

[18] G. Cesaretti, E. Dini, X. De Kestelier, V. Colla, and L. Pambaguian, Acta Astronautica, Building components for an outpost on the Lunar soil by means of a novel 3D printing technology, Acta Astronaut, vol. 93, pp. 430–450, 2014.